PHYSICAL REVIEW C VOLUME 26, NUMBER 2 AUGUST 1982

Relativistic nucleon exchange in backward p-d scattering

B. D. Keister
Department of Physics, Carnegie-Mellon University, Pittsburgh, Pennsylvania 15213

J. A. Tjon
Institute for Theoretical Physics, 3508 TA Utrecht, The Netherlands
(Received 16 April 1982)

The nucleon-exchange contribution to backward-angle *p-d* scattering is evaluated as a Feynman diagram, in which the *d-n-p* vertex function is obtained from recent numerical solutions to a bound-state Bethe-Salpeter equation. Comparisons are made to experimental cross section and polarization data, as well as to previous relativistic and nonrelativistic calculations.

[NUCLEAR REACTIONS Backward-angle *p-d* scattering and polarization. Relativistic and negative-energy effects. Bethe-Salpeter equation.]

I. INTRODUCTION

Backward-angle *p-d* scattering has been the source of hope and of disappointment in recent years.[1] The existence of a large-angle peak in the GeV energy region implies that the dominant physics might be described by the exchange of a neutron between initial and final deuterons,[2] thus suggesting that one could measure directly the high-momentum components of the deuteron wave function. Furthermore, it was found that the nucleon-exchange contribution to the *p-d* tensor polarization at 180° is directly proportional to the *D*-state wave function,[3] thus suggesting an even more sensitive way to probe high-momentum components of nucleons and excited N^*'s in the deuteron.

The realization of these ideas has been rather discouraging. There are theoretical analyses[4,5] which indicate that the nucleon-exchange picture is not necessarily the dominant mechanism. The results of experiments are also not encouraging for such simple pictures, particularly in the case of the tensor polarization, where a null measurement[6] contradicts directly a prediction of large alignment effects due to the deuteron *D* state.[3]

There have been a number of other mechanisms proposed as important for backward *p-d* scattering (see, for example, Ref. 1). Apart from the importance of other mechanisms, several authors[7–10] have investigated the possibility of relativistic effects in the nucleon-exchange diagram itself, including the contribution of the negative-energy *P* states,[7–9] as well as the transformation of the wave function from the deuteron rest frame to the three-body center of mass.[7,10] In Ref. 10, the nucleon-exchange diagram was reexamined as a Feynman diagram, with the particular aim of examining the effect of the center-of-mass transformation on the spin components of the *d-n-p* vertex function, and in turn the predicted tensor polarization. The invariant amplitudes in the *d-n-p* vertex function were identified with nonrelativistic wave functions in the deuteron rest frame, by comparing relativistic positive-energy Dirac spinor matrix elements with those of nonrelativistic Pauli spinors. It was found in Ref. 10 that the restriction to positive-energy spinors in identifying the invariant amplitudes leads to inconsistent results, even at low energy, particularly in the tensor polarization; i.e., the relativistic extension of a nonrelativistic tensor *D* wave involves coupling of positive- and negative-energy states. The question of relativistic effects thus remained unresolved, awaiting a more consistent calculation.

In this paper, we present such a consistent calculation of the nucleon-exchange contribution to backward *p-d* scattering. The invariant amplitudes in the *d-n-p* vertex function are given in terms of numerical solutions to the Bethe-Salpeter equation, in which both positive- and negative-energy components are present. The inconsistencies discussed in Ref. 10 are thus avoided. We recognize that nucleon exchange is probably not the exclusive mechanism for this reaction. Instead, our goal is to isolate the important ingredients for a consistent relativistic calculation to which one may then wish to add many other contributions. In Sec. II we outline the ingredients of the calculation, and in Secs. III and IV we discuss the results and draw conclusions.

II. DISCUSSION OF THE METHOD

Unless otherwise specified, the notation of Ref. 11 is used throughout. Using the kinematics shown in Fig. 1, the nucleon-exchange contribution to the elastic *p-d* cross section is

$$\frac{d\sigma}{d\Omega}=\frac{m^2}{s}\frac{1}{(4\pi)^2}\,|\mathscr{M}\,|^2\,, \qquad (1)$$

where m is the nucleon mass, s is the total center-of-mass energy squared, and

$$\mathscr{M}=\bar{u}(p')\Gamma(q;d)[(\not k-m)^T]^{-1}\bar{\Gamma}(q';d')u(p),$$
$$k=d-p'\,. \qquad (2)$$

Γ is the 16-component *d-n-p* vertex amplitude in the product space of two nucleon spinors, and $\bar{\Gamma}=\gamma^0\Gamma^\dagger\gamma^0$. Since the external nucleons are on the mass shell, each amplitude Γ can be described by only four independent functions[12]

$$\Gamma(q;d)=\xi_u\mathscr{J}^\mu\,, \qquad (3)$$

$$\mathscr{J}^\mu=\left\{A(q;d)\gamma^\mu+\frac{1}{m}B(q;d)q^\mu\right.$$
$$\left.+[F(q;d)\gamma^\mu+\frac{1}{m}G(q;d)q^\mu]\left[\frac{\not k+m}{2m}\right]\right\}C\,, \qquad (4)$$

where ξ^μ is the deuteron polarization vector and C is the charge conjugation matrix.

In the present work, the invariant amplitudes A, B, F, and G are extracted from recent solutions to the Bethe-Salpeter equation for Γ.[13] The kernel consists of single exchanges of η, ϵ, δ, ρ, and ω mesons, as well as pions coupled to a pseudovector vertex. This kernel sucessfully reproduces nucleon-nucleon phase shifts below the production threshold,[14] and the meson-nucleon vertex cutoff mass has been adjusted so that the observed deuteron binding energy is reproduced.

The aforementioned solutions are expressed in terms of channel amplitudes in an angular-momentum/helicity basis.[15,16] If one particle is on the mass shell, then the four channels which contribute are ${}^3S_1^+$, ${}^3D_1^+$, ${}^1P_1^-$, and ${}^3P_1^-$, corresponding to the usual S and D states, and the negative-parity P states which arise from negative-energy components of the off-shell nucleon. These channel amplitudes can in turn be related to the invariants A, B, F, and G. The details of this procedure are given in Appendix A.

At this point it is worth mentioning that the channel functions and the invariant amplitudes depend upon $|\vec{q}\,|$ *and* q_0, the nucleon relative energy. While the value of q_0 is kinematically fixed by the external momenta, it is never zero and is *real,* whereas the Wick-rotated Bethe-Salpeter solutions are functions of $|\vec{q}\,|$ and iq_4. Nevertheless, one can analytically continue the channel functions from imaginary to real relative energy by iterating the bound-state equation with the Wick-rotated solutions inserted into the integral. The result of this procedure for the deuteron is that there is very little difference ($<5\%$) between evaluating the channel functions at the appropriate value of q_0, and simply setting $q_0=0$. The calculations reported here employ the latter choice.

To obtain the cross section, one evaluates the amplitude $\mathscr{M}$ in Eq. (2) and sums over all proton and deuteron polarizations in Eq. (1). The tensor alignment $A(\theta)\equiv\sqrt{2}t_{20}(\theta)$ is obtained by calculating

$$A(\theta)=1-3\frac{d\sigma_0}{d\Omega}\bigg/\left[\frac{d\sigma_0}{d\Omega}+\frac{d\sigma_+}{d\Omega}+\frac{d\sigma_-}{d\Omega}\right], \qquad (5)$$

where ($+$, $-$, 0) are the available polarizations of the incoming deuteron. The results of the trace algebra for the cross section and tensor polarization are given in Appendix B.

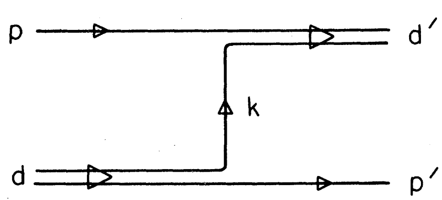

FIG. 1. The nucleon-exchange diagram, illustrating the kinematics used in the text.

III. RESULTS

The backward angle *p-d* elastic cross section prediction for the nucleon-exchange diagram evaluated with Bethe-Salpeter *d-n-p* amplitudes is shown in Fig. 2. The predicted tensor polarization at 180° is shown in Fig. 3. The agreement with the data is still rather poor, thus implying that even a consistent, relativistic calculation of the nucleon-exchange diagram is insufficient to describe the reaction.

Furthermore, one can draw conclusions about certain features of the *d-n-p* vertex function by comparing to less complete calculations. First, the contribution of the lower-component *P* states is very small, giving a maximum partial cross section of 0.1 μb/sr, and affecting the tensor polarization only by small amounts at 2 GeV incident proton energy. Recent three-dimensional calculations by Buck and Gross[17] indicate that the *P*-state component of the *d-n-p* vertex function can be enhanced by using pseudoscalar in place of pseudovector pion coupling. To study this in our case, we have generated new *P*-state components perturbatively from the positive-energy amplitudes using one-pion exchange with pseudoscalar coupling. The results using these new amplitudes are shown in Figs. 4 and 5. The cross section increases considerably due to the *P*-state components, while the tensor polarization becomes significantly smaller. The latter result comes from the dominance of the $^3P_1$ amplitude, which has a tensor polarization signature of $+1$, whereas $^1P_1$ has -2 and $^3D_1$ has -1. It should be noted, however, that this enhancement of the *P* state may

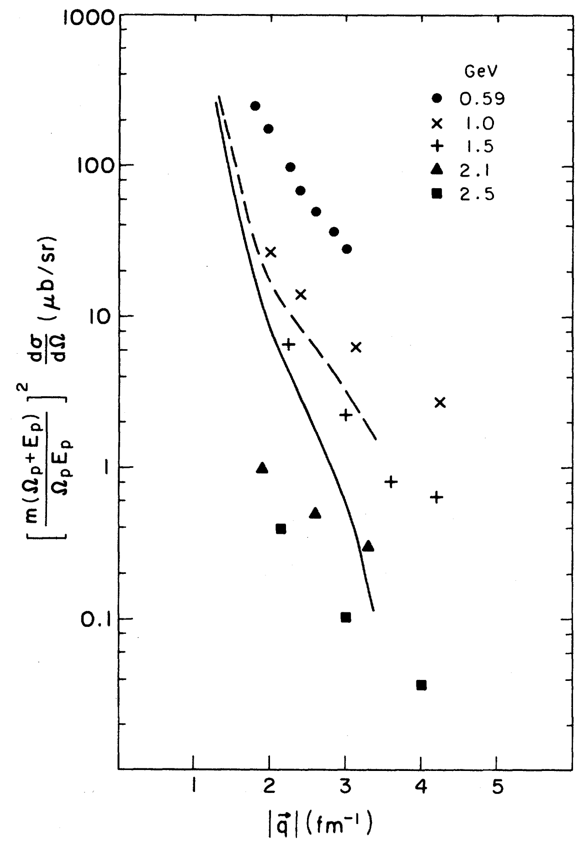

FIG. 2. Elastic *p-d* differential cross section as a function of the relative momentum *q* in the nucleon-exchange diagram. The solid line represents the calculation using the full Bethe-Salpeter calculation; the dashed line represents an old-fashioned calculation using the Bethe-Salpeter *S* and *D* states only. The data are the same as those cited in Ref. 10.

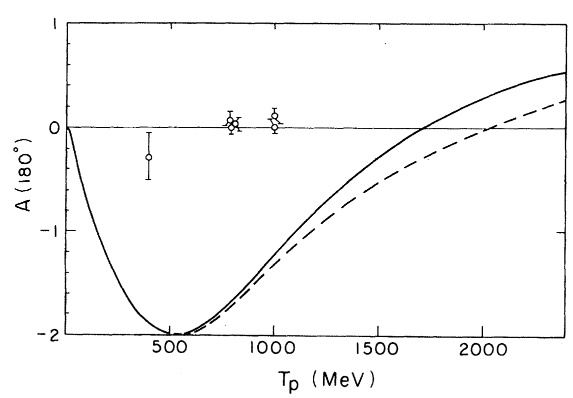

FIG. 3. Elastic *p-d* tensor alignment at 180° as a function of laboratory proton energy. The curves are the same as in Fig. 2. The data are those of Ref. 6.

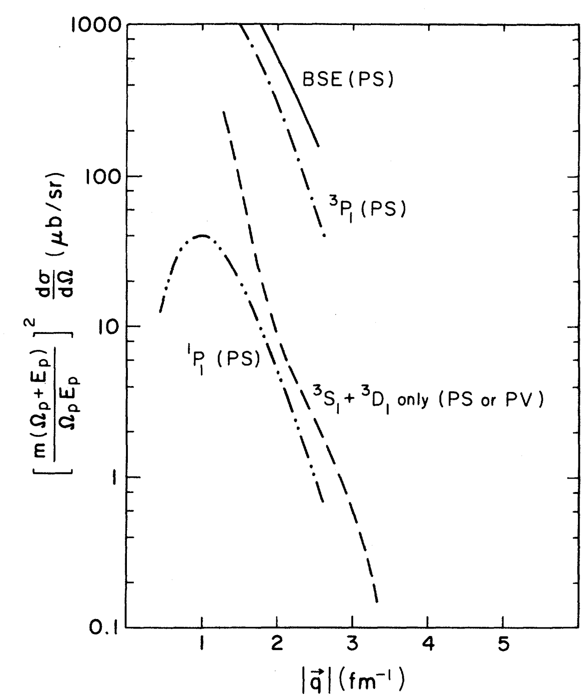

FIG. 4. Elastic *p-d* differential cross section for Bethe-Salpeter amplitudes obtained using pseudoscalar pion exchange. The solid line represents the full calculation and the dashed, dashed-dotted and dashed-double-dotted lines represent the contributions of the $^3S_1^+$, $^3D_1$, $^3P_1$ and $^1P_1$ channels, respectively.

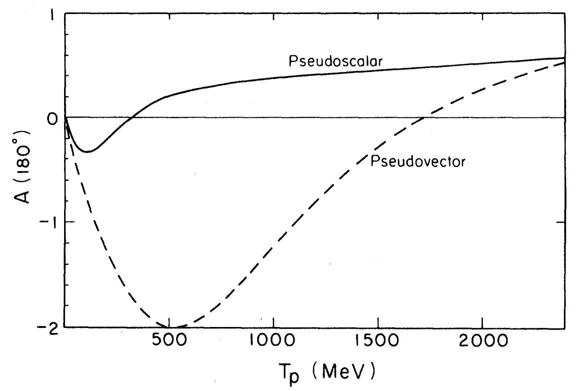

FIG. 5. Elastic *p-d* tensor alignment for Bethe-Salpeter amplitudes obtained using pseudoscalar (solid line) and pseudovector (dashed line) pion exchange.

well be canceled in backward *p-d* scattering by including certain contact terms which arise from pseudoscalar coupling by chiral symmetry.[18] Furthermore, the coupling between positive and negative energy states in the Bethe-Salpeter equation with a pseudoscalar interaction is so large that it yields very poor agreement with nucleon-nucleon phase shift data.[14] Clearly, a strong suppression of the negative-energy amplitude is needed to improve the fit. As a consequence, this may lead to significantly smaller *P*-state components in the deuteron.

Second, the relativistic calculation with Bethe-Salpeter amplitudes predicts observables which are qualitatively similar to, but quantitatively different from, old-fashioned calculations which use *S*- and *D*-state wave functions, relativistic kinematics, and two-component spin functions. As a direct test, one can identify old-fashioned *S*- and *D*-state wave functions from the Bethe-Salpeter channel amplitudes using the relations

$$\begin{aligned} w_0(q) &= \phi(^3S_1)/Z \ , \\ w_2(q) &= \phi(^3D_1)/Z \ , \\ Z &= (16\pi M_D)^{1/2}(2E_q - M_D) \ . \end{aligned} \tag{6}$$

The relative three-momentum q is evaluated in the deuteron rest frame. The old-fashioned expressions for the cross section and polarization are

$$\begin{aligned} \frac{d\sigma}{d\Omega} &= 3[q^2 + mE]^2[\Omega_p E_p/(\Omega_p + E_p)]^2 \\ &\quad \times [w_0^2(q) + w_2^2(q)]^2 \ , \\ A(180^\circ) &= \frac{[2\sqrt{2}w_0(q) - w_2(q)]w_2(q)}{w_0^2(q) + w_2^2(q)} \ . \end{aligned} \tag{7}$$

From Figs. 2 and 3, we observe that the old-fashioned and exact Bethe-Salpeter calculations are qualitatively similar, although the cross sections differ by a factor of 3 and the polarizations differ somewhat for relative momenta $q \sim m/2$. These results imply that spin-dependent boost effects are small, but that spin-independent boost effects can modify the cross section substantially at higher energies. The old-fashioned Bethe-Salpeter results are also similar to those obtained from old-fashioned calculations using the Reid[19] or Paris[20] potentials, because the wave functions $w_L(q)$ are quite similar in all three cases.[13]

A closer examination of our results also indicates that negative-energy components still play an important role in the relativistic calculation, even if the *P*-state contributions are small. While the amplitudes F and G are generally considered to represent negative-energy effects in the deuteron, we note that G is not zero even when both *P* states vanish (cf. Appendix A). If G is arbitrarily set to zero in the relativistic calculation, then we reproduce the results which one would get by using the procedure of Ref. 10, namely by ignoring the amplitudes F and G, and by identifying A and B in terms of *S*- and *D*-state wave functions. Thus, the inclusion of lower-component effects through the amplitude G provides the remaining boost effect in the cross section and is crucial for calculating the tensor polarization in a consistent manner, even though the boost effects for $A(\theta)$ are small.

We can now summarize the role of relativistic effects in the nucleon-exchange diagram. By far the most important element is the use of the relative momentum variable q in the deuteron rest frame, rather than the variable Δ in the three-body center of mass as noted by Noble and Weber.[4] It then appears that the results using the full Bethe-Salpeter amplitude with pseudovector pion exchange can be reproduced by identifying the amplitudes A, B, *and* G in terms of the wave functions $w_0(q)$ and $w_2(q)$, using Eqs. (6) and (A6). Using the wave functions of the Reid or Paris potentials in this manner would also give similar results. The boost effects, correctly included in the relativistic calculation, affect primarily the cross section magnitude and not the tensor polarization. On the other hand, the *P* states can be very important if pseudoscalar pion coupling is used, but it is not clear that this result is consistent with chiral symmetry or nucleon-nucleon scattering data.

IV. SUMMARY

We have calculated the nucleon-exchange contribution to backward *p-d* elastic scattering as a relativistic Feynman diagram. The *d-n-p* vertex functions are described in terms of recent numerical solutions to the bound-state Bethe-Salpeter equation. As is the case for the nonrelativistic calculation, the agreement with the experimental cross section and polarization data is still rather poor, indicating unambiguously that the nucleon-exchange diagram alone is not sufficient to describe the physics of backward *p-d* scattering. However, apart from the disagreement with experiment, we can use the exact nucleon-exchange calculations to test various approximate relativistic and nonrelativistic calculations. Assuming that the correct relativistic kinematics is used, the main relativistic effect is a normalization factor due to a boost of the *d-n-p* vertex function from the deuteron rest frame to the three-body center of mass. Spin-dependent boost effects are much less important. However, the relativistic calculation depends crucially upon negative-energy contributions for consistent results. The *P*-state contributions are very small or very large when pseudovector or pseudoscalar pion exchange is employed in the Bethe-Salpeter equation, though the pseudovector results are preferred for several different physical reasons.

ACKNOWLEDGMENTS

One of us (B.D.K.) wishes to thank Professor F. Gross for several helpful discussions. He also acknowledges financial support for this work from the U.S. National Science Foundation.

APPENDIX A: INVARIANT AMPLITUDES

In this Appendix we give expressions for the invariant *d-n-p* amplitudes *A*, *B*, *F*, and *G* in terms of numerical solutions for angular momentum channel functions ${}^3S_1^+$, ${}^3D_1^+$, ${}^1P_1^-$, and ${}^3P_1^-$.

It is convenient to work with a helicity spinor basis defined along the *z* axis as follows:

$$u_\lambda(q)\equiv\begin{bmatrix}1\\ \dfrac{2q\lambda}{E_q+m}\end{bmatrix}N_qX_\lambda,$$
$$v_\lambda(q)\equiv\begin{bmatrix}-\dfrac{2q\lambda}{E_q+m}\\ 1\end{bmatrix}N_qX_{-\lambda}\ , \qquad (A1)$$

where $E_q\equiv(q^2+m^2)^{1/2}$, $\lambda=\pm1$ is the helicity, and X_λ are the usual Pauli spinors. The normalization

$$N_q=[(E_q+m)/2E_q]^{1/2}$$

differs from Ref. 11 by a factor of $(E_q/m)^{1/2}$.

We consider the deuteron in its rest frame. The nucleons have momenta p^μ and k^μ, where $p^0=E_p$, k^μ is off shell, and $\vec{p}=-\vec{k}=\vec{q}$. We then define helicity spinors for each nucleon

$$\begin{aligned}U_{\lambda_p}^{(+)}(p)&=u_{\lambda_p}(q)\\ U_{\lambda_p}^{(-)}(p)&=v_{-\lambda_p}(-q)\ .\\ U_{\lambda_k}^{(+)}(k)&=u_{-\lambda_k}(-q),\\ U_{\lambda_k}^{(-)}(k)&=v_{\lambda_k}(q)\ ,\end{aligned}\qquad (A2)$$

where $\rho=\pm1$ denotes a positive- or negative-energy state, and $\lambda=\lambda_p-\lambda_k$ is the total helicity. If $\vec{p}$ makes an angle θ with the *z* axis, the rotated spinors are obtained via the transformation

$$R(\theta)=\exp(-i\theta\sigma_2/2)\ .$$

The angular momentum channel functions are obtained by projecting the 16-component vertex function onto this helicity basis:

$$\Phi^{(m)}_{\substack{\rho_p\lambda_p\\ \rho_k\lambda_k}}(\vec{q})=\bar{U}^{\rho_p}_{\lambda_p}(\vec{p})\Gamma^{(m)}(q;d)\bar{U}^{\rho_k}_{\lambda_k}(\vec{k})^T\ , \qquad (A3)$$

where (m) is the deuteron polarization. Decomposing Φ into states of total *L*, *S*, and *J*, we get[16]

$$\Phi^{(m)}_{\substack{\rho_p\lambda_p\\ \rho_k\lambda_k}}(\vec{q})=\sum_\alpha\left[\frac{2L+1}{2}\right]^{1/2}\left\langle LOS\frac{\lambda}{2}\middle|J\frac{\lambda}{2}\right\rangle\left\langle\frac{1}{2}\frac{\lambda_p}{2}\frac{1}{2}-\frac{\lambda_k}{2}\middle|S\frac{\lambda}{2}\right\rangle d^{(J)*}_{m\frac{\lambda}{2}}(-\theta)\phi(|\vec{q}|,q_0\alpha), \qquad (A4)$$

where the *d* function follows the notation of Edmonds.[21] The channel index $\alpha=1$, 2, 3, and 4 corresponds to ${}^3S_1^+$, ${}^3D_1^+$, ${}^1P_1^-$, and ${}^3P_1^-$, respectively. These channels can be projected by setting $m=0$, $\rho_p=\lambda_p=+1$, and letting $(\rho_k,\lambda_k)=(+,+)$, $(+,-)$, $(-,+)$, and $(-,-)$, on both sides of Eq. (A3). This yields the following relations:

$$-\frac{m}{E}A+\frac{q^2}{mE}B+\frac{(k^0-E)}{2m}F=-\tfrac{1}{2}\phi(^3S_1)+\frac{1}{\sqrt{2}}\phi(^3D_1)\,,$$
$$-A+\frac{1}{2E}(k^0-E)F=-\tfrac{1}{2}\phi(^3S_1)-\frac{1}{\sqrt{8}}\phi(^3D_1)\,,$$
$$\frac{q}{E}A+\frac{q}{E}B+\frac{q}{2m^2}(k^0+E)G=-(\tfrac{3}{4})^{1/2}\phi(^1P_1)\,,$$
$$\frac{q}{2mE}(k^0+E)F=(\tfrac{3}{8})^{1/2}\phi(^3P_1)\,. \tag{A5}$$

Inverting these relations gives the desired expressions for the invariant amplitudes

$$F=(\tfrac{3}{8})^{1/2}\frac{2mE}{q(k^0+E)}\phi(^3P_1)\,,$$
$$A=\tfrac{1}{2}\phi(^3S_1)+\frac{1}{\sqrt{8}}\phi(^3D_1)+(\tfrac{3}{8})^{1/2}\frac{m}{q}\left[\frac{k^0-E}{k^0+E}\right]\phi(^3P_1)\,,$$
$$B=\frac{mE}{q^2}\left[-\frac{1}{2}\left[\frac{E-m}{E}\right]\phi(^3S_1)+\frac{1}{\sqrt{8}}\left[\frac{2E+m}{E}\right]\phi(^3D_1)-(\tfrac{3}{8})^{1/2}\frac{E}{q}\left[\frac{k^0-E}{k^0+E}\right]\phi(^3P_1)\right]\,,$$
$$G=\frac{2m^2}{q(k^0+E)}\left[-\frac{q}{E}(A+B)-(\tfrac{3}{4})^{1/2}\phi(^1P_1)\right]\,. \tag{A6}$$

The channel functions have been obtained by solving the homogeneous Bethe-Salpeter equation. To be consistent with Eqs. (1) and (2) in the text, the normalization of the solution is chosen such that

$$\sum_n P_n=1\,, \tag{A7}$$

with

$$P_n=\frac{1}{16\pi^3 M_D}\int_{-\infty}^{\infty}dp_4\int_0^{\infty}p^2dp\left[\frac{\partial}{\partial E}S(p,p_4,n)\right]_{E=1/2M_D}|\phi_n(p,p_4)|^2\,, \tag{A8}$$

where we have used the notation of Ref. 13. $S(p,p_4,n)$ is the channel-decomposed two-nucleon propagator. The "probabilities" P_n for our solution are found to be $P(D^+)=4.8\%$, $P(D^-)=-6\times10^{-4}\%$, $P(^1P_1)=-2.5\times10^{-2}\%$, and $P(^3P_1)=-8.8\times10^{-3}\%$ (note that there is an error in Table II of Ref. 13).

APPENDIX B: TRACE CALCULATIONS

In this appendix we present the results of the cross section and polarization calculations. The unpolarized cross section is

$$\frac{d\sigma}{d\Omega}=\frac{m^2}{(4\pi)^2 s}\frac{1}{6}\sum_{\text{spins}}|\mathcal{M}|^2\,, \tag{B1}$$

where

$$\sum_{\text{spins}}|\mathcal{M}|^2=\sum_{\text{spins}}\bar{u}(p')\xi^*_\mu\mathcal{F}^\mu[(\not{k}-m)^{-1}]^T \times\xi'_\nu\overline{\mathcal{F}}'^\nu u(p) \times\bar{u}(p)\xi'^*_\rho\mathcal{F}'^\rho[(\not{k}-m)^{-1}]^T \times\xi_\sigma\overline{\mathcal{F}}^\sigma u(p')\,. \tag{B2}$$

The unprimed (primed) quantities refer to the incoming (outgoing) deuteron, and the ξ^μ are deuteron polarization vectors boosted to the three-body center of mass, with the property

$$\sum_{\text{spins}} \xi_\mu^* \xi_\sigma = -g_{\mu\sigma} + d_\mu d_\sigma / M_D{}^2 \ . \qquad \text{(B3)}$$

We now define projected vectors

$$Q^\mu \equiv q^\mu - d^\mu (q\cdot d)/M_D{}^2 \ ,$$
$$p'^\mu \equiv p'^\mu - d^\mu (p'\cdot d)/M_D{}^2 \ , \qquad \text{(B4)}$$

as well as a similar pair obtained by reversing primed and unprimed quantities. We then construct a special four-vector

$$S_\mu \equiv A^2(2P'_\mu - 3p'_\mu) + B^2 \frac{Q^2}{m^2} p'_\mu + 2ABQ_\mu + AF(2P'_\mu - 3p'_\mu + 3k_\mu) + BG\frac{Q^2}{m^2}(p'_\mu + k_\mu)$$
$$+(AG+BF)\left(Q_\mu + \frac{(Q\cdot p')}{m^2}k_\mu\right) + \frac{(AG-BF)}{m^2}[(p'\cdot k)Q_\mu - (Q\cdot k)p'_\mu]$$
$$+\frac{F^2}{4m^2}[2(P'\cdot k)k_\mu - 6(p'\cdot k)k_\mu + (m^2-k^2)(2P'_\mu - 3p'_\mu) + 6m^2 k_\mu]$$
$$+G^2\frac{Q^2}{4m^4}[2(p'\cdot k)k_\mu + (m^2-k^2)p'_\mu + 2m^2k_\mu]$$
$$+FG/4m^3[4m(Q\cdot p')k_\mu + 4m(Q\cdot k)k_\mu + 2m(m^2-k^2)Q_\mu] \ . \qquad \text{(B5)}$$

The vector S_μ is obtained by reversing primed and unprimed quantities, with $k'_\mu = k_\mu$. Finally, we construct a Lorentz scalar

$$T \equiv 3mA^2 + B^2Q^2/m^2 + 2AB\frac{(Q\cdot p')}{m} + AF\left[\frac{2(p'\cdot k)}{m} - 3\frac{(p'\cdot k)}{m} + 3m\right] + BG\frac{Q^2}{m^2}\left[\frac{(p'\cdot k)}{m} + m\right]$$
$$+(AG+BF)\left[\frac{(Q\cdot k)}{m} + \frac{(Q\cdot p')}{m}\right] + \frac{F^2}{4m^2}[4m(P'\cdot k) - 6m(p'\cdot k) + 3m(k^2+m^2)]$$
$$+G^2\frac{Q^2}{4m^4}[2m(p'\cdot k) + m(k^2+m^2)] + \frac{FG}{4m^3}[2(k^2+m^2)(Q\cdot p') + 4m^2(Q\cdot k)] \ . \qquad \text{(B6)}$$

The spin sum is then

$$\sum_{\text{spins}} |\mathcal{M}|^2 = 4[2m(k^2-m^2)]^{-2}\{(k^2-m^2)[T^2 - (S\cdot S')] + 2[mT - (k\cdot S)]^2\} \ . \qquad \text{(B7)}$$

For the tensor polarization, we need only calculate $\sum_{\xi';s;s'} |\mathcal{M}|^2$, where only the incoming deuteron spin is not summed, having been fixed at its longitudinal value, $\xi^{(0)} \equiv (0,0,0,1)$ in the rest frame.

We define an additional four-vector

$$U_\mu \equiv A^2[2(\xi\cdot p')\xi_\mu + p'_\mu] + B^2\frac{(q\cdot\xi)^2}{m^2}p'_\mu + 2AB(q\cdot\xi)\xi_\mu$$
$$+AF[2(\xi\cdot p')\xi_\mu + p'_\mu - k_\mu] + BG\frac{(q\cdot\xi)^2}{m^2}[p'_\mu + k_\mu]$$
$$+(AG+BF)(q\cdot\xi)\left[\xi_\mu + \frac{(\xi\cdot p')}{m^2}k_\mu\right] + (AG-BF)\frac{(q\cdot\xi)}{m^2}[(k\cdot p')\xi_\mu - (\xi\cdot k)p'_\mu]$$
$$+\frac{F^2}{4m^2}[4(\xi\cdot p')(\xi\cdot k)k_\mu + 2(p'\cdot k)k_\mu + 2(\xi\cdot p')(m^2-k^2)\xi_\mu + (m^2-k^2)p'_\mu - 2m^2k_\mu]$$
$$+G^2\frac{(q\cdot\xi)^2}{4m^4}[2(p'\cdot k)k_\mu + (m^2-k^2)p'_\mu + 2m^2k_\mu]$$
$$+FG\frac{(q\cdot\xi)}{4m^3}[4m(\xi\cdot p')k_\mu + 4m(\xi\cdot k)k_\mu + 2m(m^2-k^2)\xi_\mu] \ , \qquad \text{(B8)}$$

and an additional scalar

$$V \equiv -mA^2+B\frac{(q\cdot\xi)^2}{m}+2AB\frac{(q\cdot\xi)(\xi\cdot p')}{m}+AF\left[\frac{2(\xi\cdot p')(\xi\cdot k)}{m}+\frac{(k\cdot p')}{m}-m\right]$$
$$+BG\frac{(q\cdot\xi)^2}{m^2}\left[\frac{(k\cdot p')}{m}+m\right]+(AG+BF)(q\cdot\xi)\left[\frac{(k\cdot\xi)}{m}+\frac{(\xi\cdot p')}{m}\right]$$
$$+\frac{F^2}{4m^2}[4m(\xi\cdot p')(\xi\cdot k)+2m(p'\cdot k)-m(k^2+m^2)] \tag{B9}$$
$$+G^2\frac{(q\cdot\xi)^2}{4m^4}[2m(p'\cdot k)+m(k^2+m^2)]$$
$$+FG\frac{(q\cdot\xi)}{4m^3}[2(\xi\cdot p')(k^2+m^2)+4m^2(\xi\cdot k)] .$$

The tensor alignment is then

$$A=1-3N_0/(N_+ +N_- +N_0) , \tag{B10}$$

where

$$\frac{N_0}{N_+ +N_- +N_0}=\sum_{\xi';s;s'}|\mathscr{M}|^2\Big/\sum_{\text{spins}}|\mathscr{M}|^2 , \tag{B11}$$

and

$$\sum_{\xi';s;s'}|\mathscr{M}|^2=-4[2m(k^2-m^2)]^{-2}\{(k^2-m^2)[TV-(S'\cdot U)+2[mT-(k\cdot S')][mV-(k\cdot U)]\} . \tag{B12}$$

[1]See, for example, L. S. Kisslinger, in *Mesons in Nuclei,* edited by M. Rho and D. Wilkinson (North-Holland, Amsterdam, 1978), p. 263, and references therein.
[2]A. K. Kerman and L. S. Kisslinger, Phys. Rev. 180, 1483 (1969).
[3]S. S. Vasan, Phys. Rev. D 8, 4092 (1973).
[4]J. V. Noble and H. J. Weber, Phys. Lett. 50B, 233 (1974).
[5]M. Levitas and J. V. Noble, Nucl. Phys. A251, 385 (1975).
[6]G. J. Igo *et al.*, Phys. Rev. Lett. 43, 425 (1979).
[7]E. A. Remler, Nucl. Phys. B42, 56;69 (1972).
[8]F. Gross, in *Few-Body Dynamics,* edited by A. N. Mitra *et al.* (North-Holland, Amsterdam, 1976), p. 523.
[9]S. Morioka and T. Ueda, See Ref. 8, p. 297.
[10]B. D. Keister, Phys. Rev. C 24, 2628 (1981).
[11]J. D. Bjorken and S. D. Drell, *Relativistic Quantum Mechanics* (McGraw-Hill, New York, 1966).
[12]R. Blankenbecler and L. F. Cook, Phys. Rev. 119, 1745 (1960).
[13]M. J. Zuilhof and J. A. Tjon, Phys. Rev. C 22, 2369 (1980).
[14]J. Fleischer and J. A. Tjon, Nucl. Phys. B84, 375 (1975); Phys. Rev. D 15, 2537 (1977); D 21, 87 (1980).
[15]M. J. Zuilhof, Ph.D. thesis, University of Utrecht, 1981 (unpublished).
[16]M. Jacob and G. C. Wick, Ann. Phys. (N.Y.) 7, 404 (1959).
[17]W. Buck and F. Gross, Phys. Rev. D 20, 2361 (1979).
[18]F. Gross, private communication.
[19]R. V. Reid, Ann. Phys. (N.Y.) 50, 411 (1968).
[20]M. Lacombe *et al.*, Phys. Rev. C 21, 861 (1980).
[21]A. R. Edmonds, *Angular Momentum in Quantum Mechanics* (Princeton University Press, Princeton, 1957).